1   **Greenhouse gas emissions from river riparian wetlands: An example from the**

2   **Inner Mongolia grassland region in China**

3   **Xinyu Liu[1], Xixi Lu[1,2], Ruihong Yu[1], Hao Xue[1], Zhen Qi[1], Zhengxu Cao[1],**

4   **Zhuangzhuang Zhang[1], Tingxi Liu[3]**

5   [1] School of Ecology and Environment in Inner Mongolia University, Key Laboratory of River and

6   Lake in Inner Mongolia Autonomous Region, Hohhot 010021, Inner Mongolia Autonomous,

7   China;

8   [2] Department of Geography, National University of Singapore, 117570, Singapor;

9   [3] Inner Mongolia Water Resource Protection and Utilization Key Laboratory, Water Conservancy

10   and Civil Engineering College, Inner Mongolia Agricultural University, Hohhot, China

11   **Corresponding author:** Ruihong Yu (rhyu@imu.edu.cn) and Tingxi Liu (txliu@imau.edu.cn)

12

13   **Abstract:** Riparian wetlands play a significant role in regulating carbon and nitrogen cycles.

14   Gradual riparian wetland drying is increasingly sensitive to global warming and contributes to

15   climate change. In this study, we analyzed the emissions of carbon dioxide (CO_2), methane (CH_4),

16   and nitrous oxide (N_2O) from riparian wetlands in the Xilin River Basin to understand the role of

17   these ecosystems in greenhouse gas (GHG) emissions. Moreover, the impact of the catchment

18   hydrology and soil property variations on GHG emissions over time and space were evaluated.

19   Our results demonstrate that riparian wetlands emit larger amounts of CO_2 (335–2790 mg·m^{-2}·h^{-1}

20   in August and 72–387 mg·m^{-2}·h^{-1} in October) than CH_4 and N_2O to the atmosphere due to high

21   plant and soil respiration. The results also reveal clear seasonal variations and spatial patterns

22   along the transects and in the longitudinal direction. N_2O emissions showed a spatiotemporal

23   pattern similar to that of CO_2 emissions. Near-stream sites were the only sources of CH_4

24   emissions, while the other sites served as sinks for these emissions. Soil moisture content and soil

25   temperature were the essential factors controlling the GHG emissions, and abundant aboveground

26   biomass promoted the CO_2, CH_4, and N_2O emissions. Moreover, compared to different types of

27   grasslands, riparian wetlands were the potential hotspots of GHG emissions in the Inner

28   Mongolian region. Degradation of downstream wetlands has resulted in the loss of the soil carbon

29   pool by approximately 60%, reducing CO_2 emissions by approximately 35%, and shifting the CH_4

30   and N_2O emissions from the source to the sink. Our study showed that anthropogenic activities

31   have extensively changed the hydrological characteristics of the riparian wetlands and might

32   accelerate carbon loss, which could further affect the GHG emissions.

33

34   **Key words:** Riparian wetlands, Grasslands, Greenhouse gas, Spatial-temporal distribution, Impact

35   factor, Xilin River Basin

36

37

38

39   **1. Introduction**

40   With the increasing impacts of global warming, the change in the concentrations of

41   greenhouse gases (GHGs) in the atmosphere is a source of concern in the scientific community

42   (Cao et al., 2005). According to the World Meteorological Organization (WMO, 2018), the

43   concentrations of carbon dioxide (CO_2), methane (CH_4), and nitrous oxide (N_2O) have increased

44   by 146%, 257%, and 122%, respectively, since 1750. Despite their lower atmospheric

45   concentrations, CH_4 and N_2O absorb infrared radiation approximately 28 and 265 times more

46   effectively at centennial timescales than CO_2 (IPCC, 2013). On a global scale, CO_2, CH_4, and N_2O

47   contribute 87% to the GHG effect (Ferrón et al., 2007).

48   Wetlands are unique ecosystems that serve as transition zones between terrestrial and aquatic

49   ecosystems. They play an important role in the global carbon cycle (Beger et al., 2010; Naiman

50   and Decamps, 1997). Wetlands are sensitive to hydrological changes, particularly in the context of

51   global climate change (Cheng and Huang, 2016). Moreover, wetland hydrology is affected by

52   local anthropogenic activities, such as the construction of reservoirs, resulting in gradual drying.

53   Although wetlands cover only 4–6% of the terrestrial land surface, they contain approximately

54   12–24% of global terrestrial soil organic carbon (SOC), thus acting as carbon sinks. Moreover,

55   they release CO_2, CH_4, and N_2O into the atmosphere and serve as carbon sources (Lv et al., 2013).

56   Wetlands are increasingly recognized as an essential part of the nature, given their simultaneous

57   functions as carbon sources and sinks. Excessive rainfall will cause an expansion in wetland areas

58   and a sharp increase in the soil moisture content (SMC), thus enhancing respiration,

59   methanogenesis, nitrification, and denitrification rates (Mitsch et al., 2009). On the contrary,

60   reduced precipitation or severe droughts will result in a decrease in water levels, causing the

61 wetlands to dry up. The accumulated carbon will be released back into the atmosphere through

62 oxidation. Due to the increasing impact of climate change and human activity, the drying of

63 wetlands has been widely observed in recent years (Liu et al., 2006); more than half of global

64 wetlands have disappeared since 1900 (Mitsch and Gosselink, 2007), and this tendency is

65 expected to continue in the future. The loss of wetlands may directly shift the soil environment

66 from anoxic to oxic conditions, and modify the CO_2 and CH_4 source and sink functions of wetland

67 ecological systems (Waddington and Roulet, 2000; Zona et al., 2013).

68 The Xilin River Basin in China is characterized by a marked spatial gradient in SMC. It is a

69 unique natural laboratory that may be used to explore the close relationships between the

70 spatiotemporal variations in hydrology and riparian biogeochemistry. Wetlands around the Xilin

71 River play an irreplaceable role with regard to local climate control, water conservation, the

72 carbon and nitrogen cycles, and husbandry (Gou et al., 2015; Kou, 2018). Moreover, the Xilin

73 River region is subjected to seasonal alterations in precipitation and temperature regimes, and

74 construction of the Xilin River Reservoir has resulted in highly negative consequences, such as the

75 drying of downstream wetlands, affecting riparian hydrology as well as microbial activity in

76 riparian soils. GHG emissions in riparian wetlands vary immensely. Understanding the

77 interactions between GHG emissions and hydrological changes in the Xilin River riparian

78 wetlands has thus become increasingly important. Moreover, it is necessary to estimate the

79 changes in GHG emissions as a result of wetland degradation at the local and global scales.

80 In this work, GHG emissions from riparian wetlands and adjacent hillslope grasslands of the

81 Xilin River Basin were investigated. GHG emissions, soil temperature (ST), and SMC were

82 measured in dry and wet seasons. The main objectives of this study were to (1) investigate the

83 temporal and spatial variations in CO_2, CH_4, and N_2O emissions from the wetlands in the riparian

84 zone, and examine the main factors affecting the GHG emissions, (2) compare the GHG emissions

85 from the riparian wetlands and different types of grasslands, and (3) evaluate the impact of

86 wetland degradation in the study area on GHG emissions.

87

88 **2. Materials and methods**

89 **2.1 Study site**

90 The Xilin River is situated in the southeastern part of the Inner Mongolia Autonomous

Biogeosciences Open Access
Discussions
EGU

91   Region in China (E115°00'–117°30', N43°26'–44°39'). It is a typical inland river of the Inner

92   Mongolia grasslands. The river basin area is 10,542 km², the total length is 268.1 km, and the

93   average altitude is 988.5 m. According to the meteorological data provided by the Xilinhot

94   Meteorological Station (Xi et al., 2017; Tong et al., 2004), the long-term annual mean air

95   temperature is 1.7°C, and the maximum and minimum monthly means are 20.8°C in July and

96   −19.8°C in January, respectively. The average annual precipitation was 278.9 mm for the period of

97   1968–2015. Precipitation is distributed unevenly among the seasons, with 87.41% occurring

98   between May and September.

99   Soil types in the Xilin River Basin are predominantly chernozems (86.4%), showing a

100   significant zonal distribution as light chestnut soil, dark chestnut soil, and chernozems from the

101   northwest to southeast. Soil types in this basin also present a vertical distribution with elevation.

102   The chernozems are primarily soluble chernozems and carbonate chernozems, distributed at

103   altitudes above 1350 m with a relatively fertile and deep soil layer. Dark chestnut soil, boggy soil,

104   and dark meadow with high humus content are distributed between the altitudes of 1150 and 1350

105   m. Light chestnut soil, saline meadow soil, and meadow solonchak with low soil humus, a thin

106   soil layer, and coarse soil texture are distributed between the altitudes of 902 and 1150 m (Xi et al.,

107   2017).

108   **2.2 Field measurements and laboratory analyses**

109   In this study, five representative transects were selected as the primary measurement sites in

110   the entire Xilin River. Each transect cuts through the riparian wetlands near the river and hillslope

111   grasslands further away from it (Fig. 1).
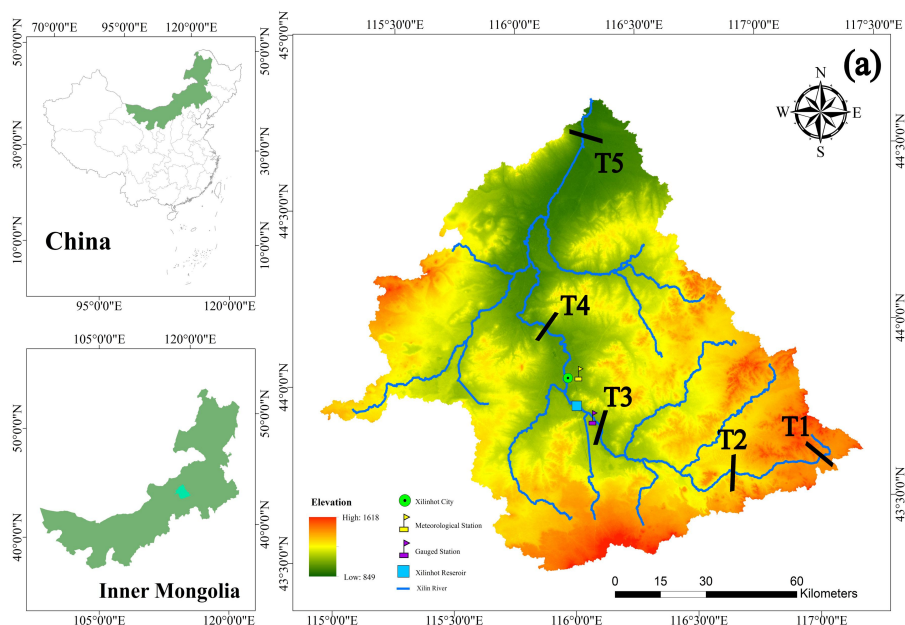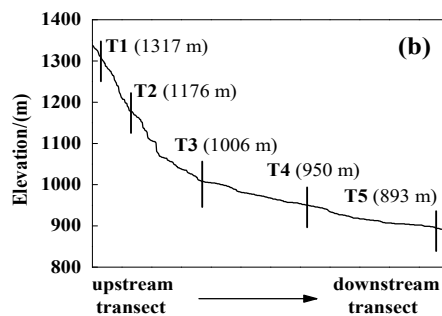
Fig. 1 (a) Location of the Xilin River Basin and distribution of five riparian-hillslope transects (T1–T5). (b) Elevation details of each transect in the Xilin River Basin.

The layout of the sampling points of each transect is shown in Fig. 2. Each sampling point for T1–T5 was extended from the river to both sides, to the grassland on the slopes, using 5–7 sampling points for each transect and resulting in 24 points in total. The sampling sites on the left and right banks were defined as L1–L3 and R1–R4 from the riparian wetlands to the hillslope grasslands. As transect T3 was located on a much wider flood plain, none of its sampling points were located on the hillslope grassland. The last transect (T5) was located downstream in the dry lake and contained seven sampling points. They were defined as S1–S7, where S1, S2, and S7

5

124 were located along the lake shore (the lakeside zone), and S3–S6 were located in the dry lake bed

125 (S3 and S4 in the mudbank, S5 in saline–alkali soil, and S6 in sand–gravel geology). Moreover,

126 characterizations for T1, T2, and T3 transects were the continuous river flow and T4 and T5

127 transects were the intermittent river flow.

128 The CO_2, CH_4, and N_2O emissions from each site were measured in August (wet season) and

129 October (dry season) in 2018 using a static dark chamber and the gas chromatography method.

130 The static chambers were made of a cube-shaped polyvinyl chloride (PVC) pipe (dimensions: 0.4

131 m × 0.2 m × 0.2 m). A battery-driven fan was installed horizontally inside the top wall of the

132 chamber to ensure proper air mixing during measurements. To minimize heating from solar

133 radiation, white adiabatic aluminum foil was used to cover the entire aboveground portion of the

134 chamber. During measurements, the chambers were driven into the soil to ensure airtightness and

135 connected with a differential gas analyzer (Li-7000 CO_2/H_2O analyzer, LI-COR, USA) to measure

136 the changes in the soil CO_2 concentration. The air in the chamber was sampled using a 60 mL

137 syringe at 0, 7, 14, 21, and 28 min. The gas samples were stored in the reservoir bag and taken to

138 the laboratory for CH_4 and N_2O measurements using gas chromatography (GC-2030, Japan). The

139 measurements were scheduled for 9:00–11:00 a.m. and 3:00–5:00 p.m.

140 ST was measured at depths of 0–10 cm and 10–20 cm with a geothermometer (DTM-461,

141 Hengshui, China). Plant samples were collected in a static chamber and over-dried in the

142 laboratory to obtain aboveground biomass (BIO). A 100 cm^3 ring cutter was used to collect surface

143 soil samples at each site, which were placed in aluminum boxes and immediately brought back to

144 the laboratory to measure SMC and soil bulk density (ρ_b) using national standard methods

145 (NATESC, 2006). Topsoil samples were collected, sealed in plastic bags, and brought back to the

146 laboratory to measure soil pH, electrical conductivity (EC), total soil organic carbon (TOC), and
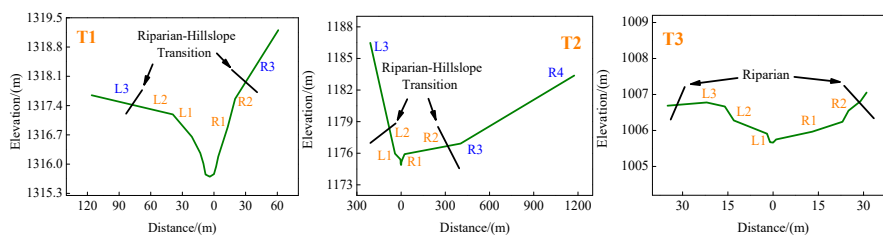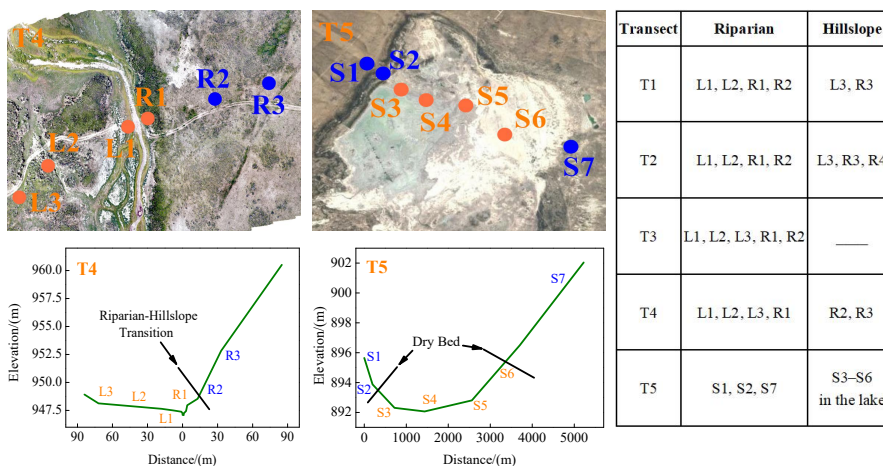
147 soil C:N ratio.

148

149
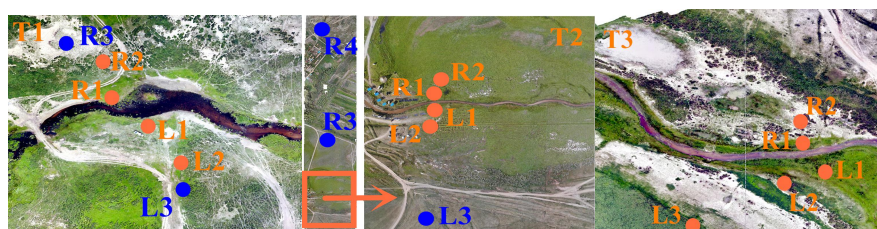
Fig. 2 Distributions of sampling points in transects T1–T5 (The images are authors' own)

Table 1. Physical and chemical properties of soils at various sites within each transect

Transect	Zone	Soil C:N	TOC (g·kg⁻¹)	BIO (g)	ρ_b	pH	EC (μs/cm)
T1	Riparian	12.46 ± 0.91	30.16 ± 6.54	14.67 ± 5.44	1.28 ± 0.07	7.25 ± 0.62	154.71 ± 23.70
	Hillslope	11.41 ± 0.09	10.77 ± 4.72	6.70 ± 1.48	1.45 ± 0.03	7.22 ± 0.40	82.02 ± 16.37
T2	Riparian	11.70 ± 1.14	19.96 ± 5.71	24.76 ± 9.65	1.23 ± 0.05	8.95 ± 0.45	303.88 ± 102.16
	Hillslope	9.77 ± 0.88	14.87 ± 11.21	6.10 ± 3.19	1.38 ± 0.13	8.10 ± 0.55	162.97 ± 128.18
T3	Riparian	16.02 ± 3.74	25.16 ± 10.25	26.65 ± 40.64	1.09 ± 0.54	9.28 ± 0.72	1067.15 ± 813.13
T4	Riparian	12.52 ± 2.06	9.96 ± 1.25	11.97 ± 4.50	1.30 ± 0.08	8.84 ± 0.22	461.72 ± 314.27
	Hillslope	9.97 ± 0.50	9.65 ± 1.05	7.84 ± 2.48	1.30 ± 0.09	8.23 ± 0.14	118.5 ± 8.25
T5	Lake shore	63.74 ± 12.93	31.41 ± 6.55	5.48 ± 2.35	1.16 ± 0.10	9.88 ± 0.18	7320.87 ± 4300.03
	Dry lake bed	15.92 ± 4.71	6.35 ± 1.16	0	1.33 ± 0.09	9.41 ± 0.7	281.82 ± 162.73

Note: Soil C:N - soil carbon-nitrogen ratio; TOC - total soil organic carbon; BIO - aboveground

biomass; ρ_b - soil bulk density; pH - soil pH; EC - soil electrical conductivity

158

2.3 Calculation of GHG emissions

160   The CO_2, CH_4, and N_2O emissions were calculated using Eq. 1 (Qin et al., 2016):

161
$$F = \frac{V}{A} \times \frac{dc}{dt} \times \rho = H \times \frac{dc}{dt} \times \frac{M}{V} \times \left(\frac{273.15}{273.15 + t} \right)$$,   (1)

162   where F denotes the CO_2, CH_4, and N_2O emissions ($mg \cdot m^{-2} \cdot h^{-1}$), H is the height of the static

163   chamber (0.18 m), M is the relative molecular weight (44 for CO_2 and N_2O, and 16 for CH_4), V is

164   the volume of gas in the standard state (22.4 $L \cdot mol^{-1}$), dc/dt is the rate of change of the gas

165   concentration ($10^{-6} \cdot h^{-1}$), and T is the temperature in the black chamber (°C).

166

3. Results

3.1 Spatiotemporal patterns of SMC for each transect

169   The spatiotemporal pattern of SMC is illustrated in Fig. 3. Similar variations were observed

170   between soil depths of 0–10 cm and 10–20 cm in the following order: wet season (August) > dry

171   season (October) and riparian wetlands > hillslope grasslands. The average SMCs in the

172   continuous river transects in the riparian zones (31.70% in August and 18.40% in October) were

173   higher than those in the hillslope grasslands (7.82% in August and 5.06% in October). During the

174   study period, the SMC changed as the distance from the river increased, and the highest value was

175   observed at the near-stream sites (L1 and R1). SMC fluctuations were low in the intermittent

176   transect compared to the upstream transects, with a mean value of 9.50% in August and 3.35% in

177   October in the riparian areas. The mean SMC in the hillslopes was 7.07% in August and 3.63% in

178   October. In transect T5, average SMCs at the center of the lake (29.15% in August and 11.52% in

179   October) were higher than those along the lake shore (4.12% in August and 4.18% in October).

180

181

182

183
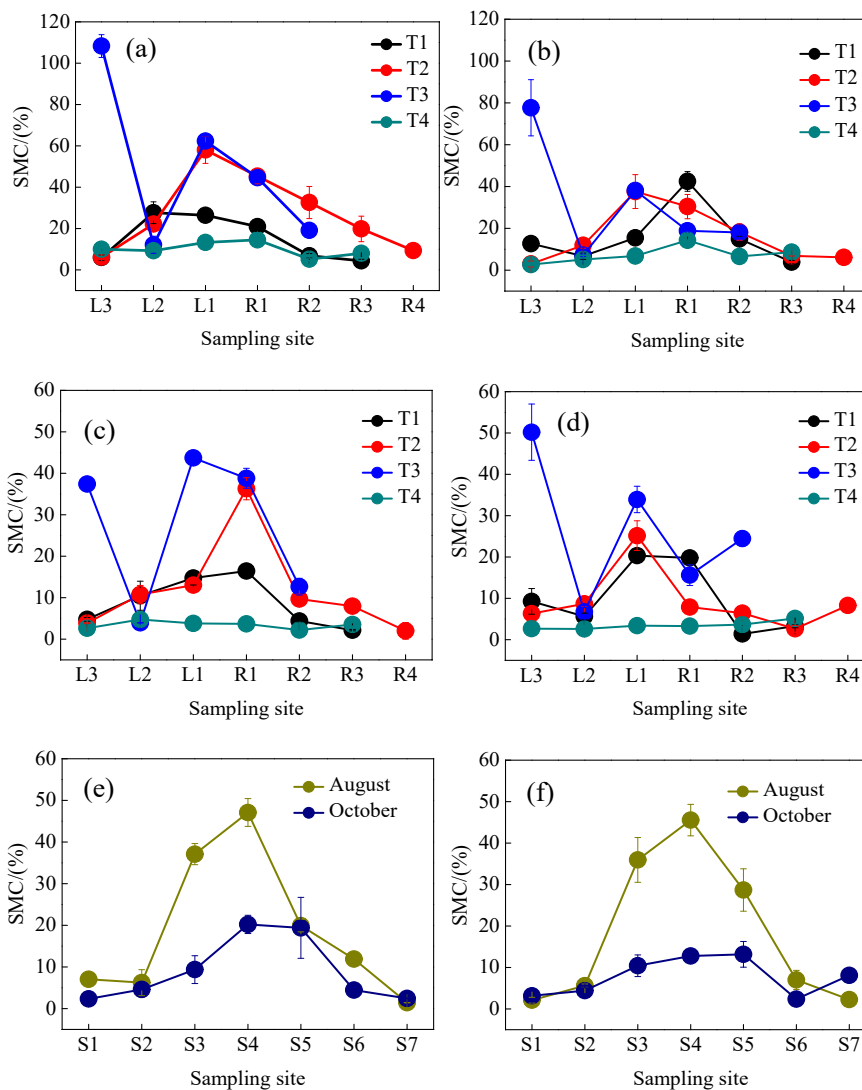
Fig. 3 Soil moisture contents (SMCs) at soil depths of 0–10 cm (SMC10) and 10–20 cm (SMC20)

for transects T1–T5 in August and October: (a) SMC10 for T1–T4 in August. (b) SMC20 for

T1–T4 in August. (c) SMC10 for T1–T4 in October. (d) SMC20 for T1–T4 in October. (e) SMC10

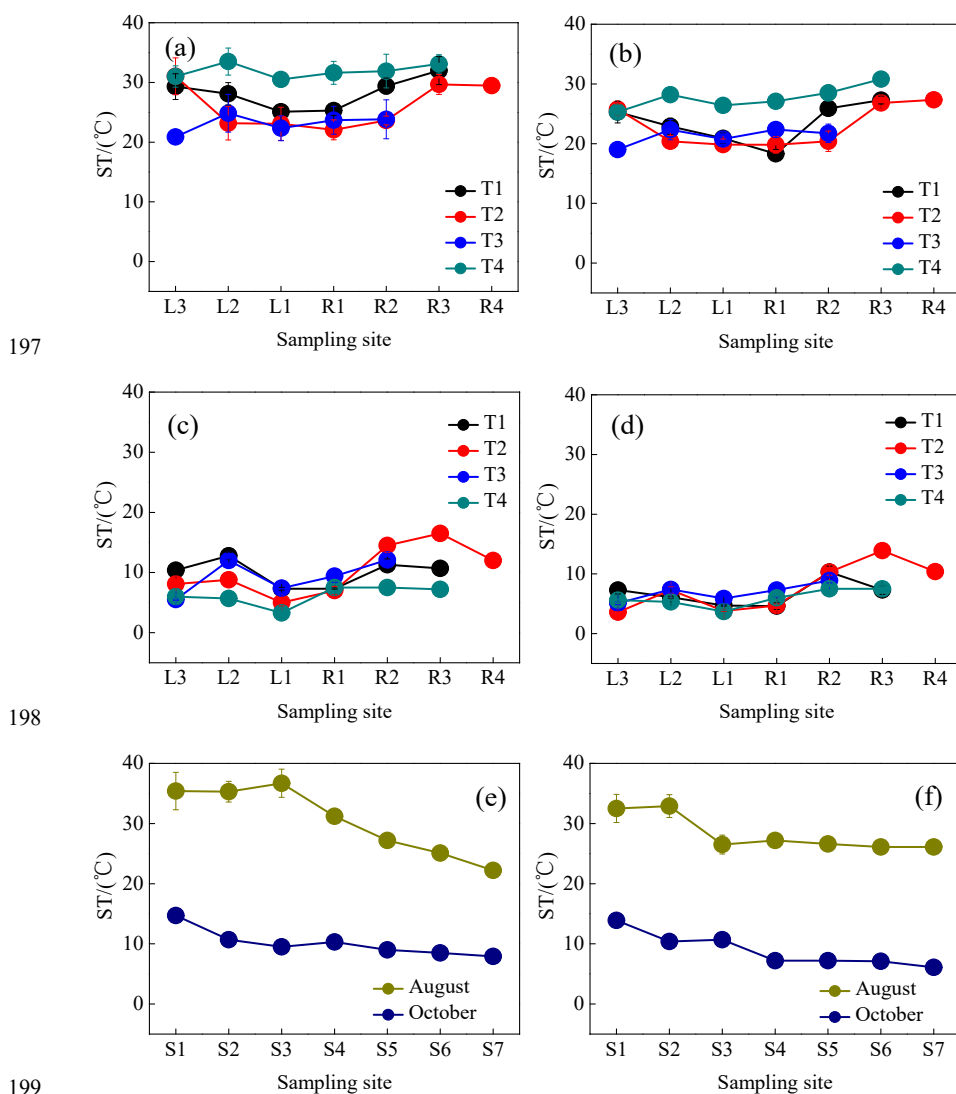for T5 in August and October. (f) SMC20 for T5 in August and October.

188

3.2 Spatiotemporal patterns of ST in each transect

Spatiotemporal differences in ST during the entire observation period are displayed in Fig. 4.

ST variations in August (mean value: 27.4°C) were noticeably higher than those in October (mean

192   value: 8.97°C). Moreover, ST for riparian sites (mean values: 26.0°C in August and 8.41°C in

193   October) was slightly lower than that for the hillslope grasslands (mean values: 30.9°C in August

194   and 10.3°C in October) for the 0–10 cm soil depth, with the exception of transect T5. Similar

195   results were observed for the 10–20 cm soil depth.

196

Fig. 4 Soil temperature (ST) at soil depths of 0–10 cm (ST10) and 10–20 cm (ST20) for transects

T1–T5 in August and October: (a) ST10 for T1–T4 in August. (b) ST20 for T1–T4 in August. (c)

ST10 for T1–T4 in October. (d) ST20 for T1–T4 in October. (e) ST10 for T5 in August and

Biogeosciences
Discussions

203   October. (f) ST20 for T5 in August and October.

204

3.3 Spatiotemporal patterns of GHG emissions in each transect

206   Figure 5 shows the spatiotemporal variations in GHG emissions in August (wet season) and

207   October (dry season) in each transect. CO_2 emissions in each transect were higher in August than

208   in October. The average emissions for the riparian wetlands of transects T1–T4 (1582.09 ± 679.34

209   mg·m^{-2}·h^{-1} in August and 163.24 ± 84.98 mg·m^{-2}·h^{-1} in October) were higher than those for the

210   hillslope grasslands (1071.54 ± 225.39 mg·m^{-2}·h^{-1} in August and 77.68 ± 25.32 mg·m^{-2}·h^{-1} in

211   October). Higher CO_2 fluxes occurred in the riparian zones, while lower CO_2 fluxes were

212   observed in the hillslope grasslands in continuous river transects (T1, T2, and T3). Transect T4

213   exhibited lower CO_2 emissions in the riparian wetlands near the channel than at sites away from

214   the channel. CO_2 emissions in transect T5 in August and October decreased from the lake shore to

215   the lake center.

216
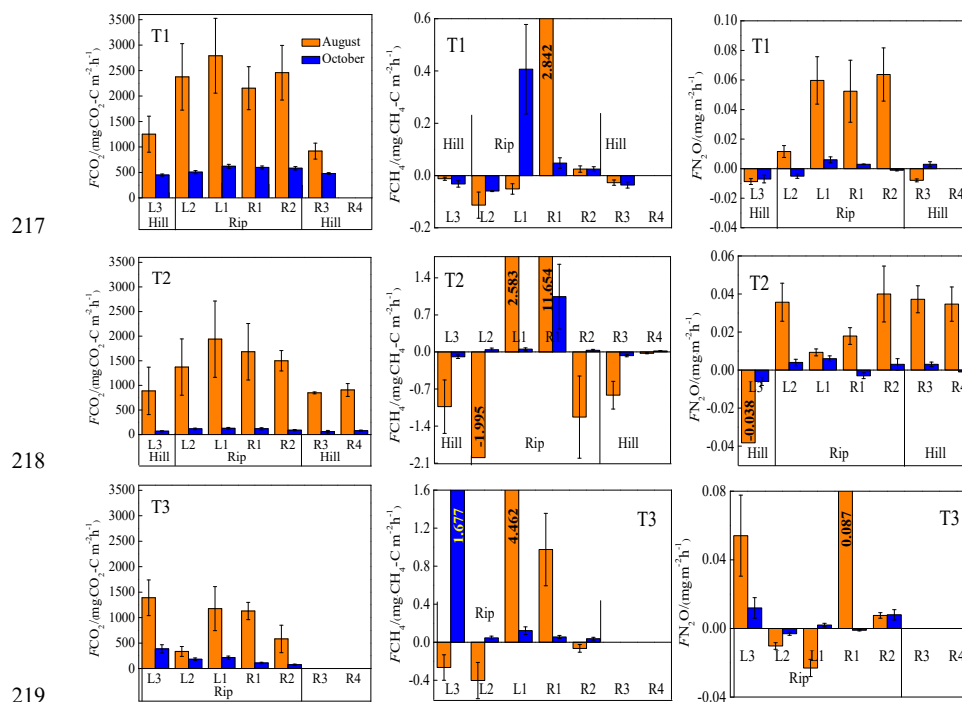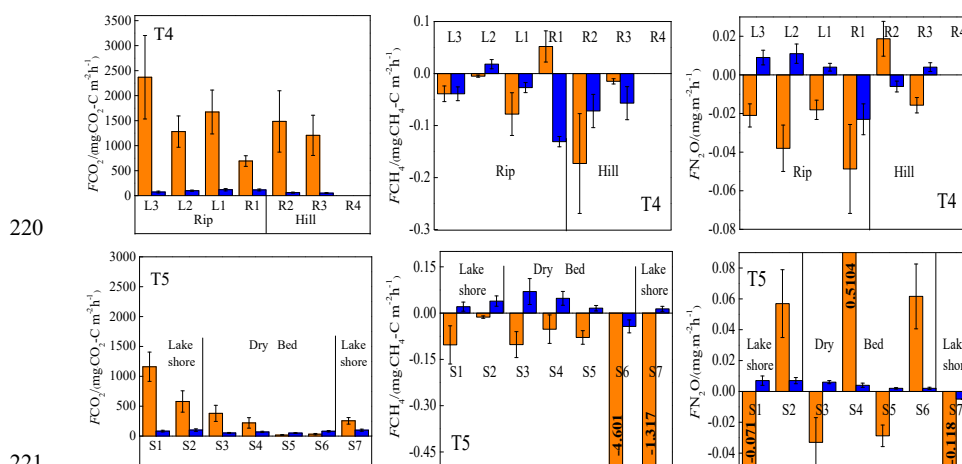
217

218

219

Fig. 5 Spatiotemporal patterns of CO_2 (first column), CH_4 (second column), and N_2O

(third column) emissions (F) for each transect. Data are shown for August (orange) and October

(blue) and error bars are the standard deviations.

CH_4 emissions at the transects with continuous river flow (T1, T2, and T3) varied between

August and October, except for T4 (characterized by intermittent river flow) and T5 (the dry lake).

In August, the near-stream sites (L1 and R1) in T1, T2, and T3 were characterized as high CH_4

sources (average: 3.74 ± 3.81 mg·m^{-2}·h^{-1}), but the sites located away from the river gradually

turned into CH_4 sinks. Moreover, all the sites in transects T4 and T5 were sinks. CH_4 emissions

(mean value: 0.2 ± 0.45 mg·m^{-2}·h^{-1}) at the wetland sites were always lower in October than those

in August. However, the sites on the hillslope grasslands served as CH_4 sinks (mean value: -0.05

± 0.03 mg·m^{-2}·h^{-1}). In transect T5, CH_4 emissions revealed the opposite trend; a CH_4 sink was

observed in August, but it was transformed into a CH_4 source in October.

Similar to the CO_2 and CH_4 emissions, N_2O emissions showed a distinct spatiotemporal

pattern for all the transects. N_2O emissions in August were higher than those in October. These

emissions were higher in riparian wetlands than in hillslope grasslands. Moreover, almost all the

sites with continuous river flow were N_2O sources, while more than half of the sites with

intermittent river flow were sinks.

3.4 Spatiotemporal patterns of GHG emissions in upstream and downstream

242 **areas**

243   Figure 6 shows the detailed spatial and seasonal distribution of GHG emissions in August and

244 October in the longitudinal direction from the upstream (T1, T2, and T3) to the downstream areas

245 (T4 and T5). The CO_2, CH_4, and N_2O emissions were calculated from the average values of the

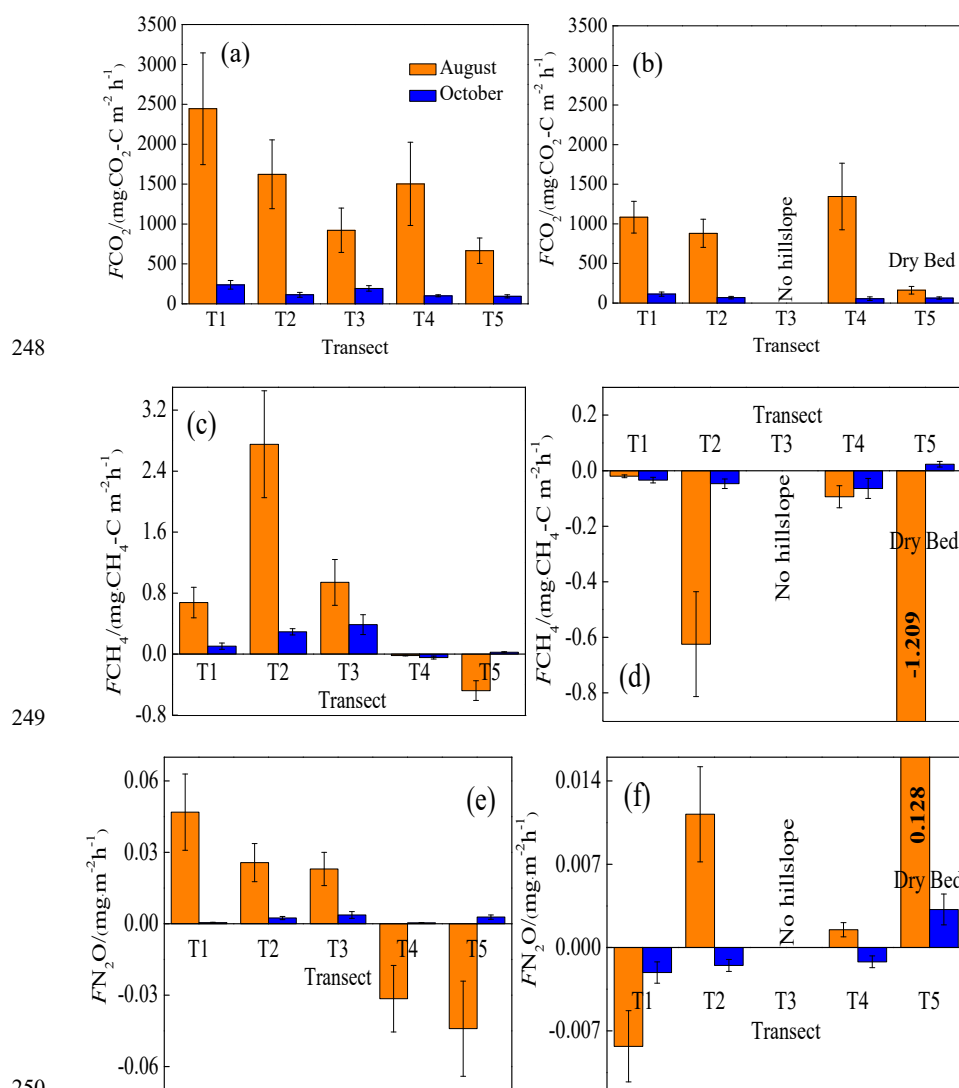246 respective emissions in the wetlands and hillslope grasslands in each transect.

247

251   Fig. 6 Spatiotemporal patterns of CO_2 (first line), CH_4 (second line), and N_2O (third line)

252   emissions (F) in the upstream (T1, T2, and T3) and downstream areas (T4 and T5). Data are

253   shown for the riparian wetlands (a, c, e) and hillslope grasslands (b, d, f) in August (orange) and

254   October (blue). Bars are the mean values for each transect and error bars are the standard errors.

255

256   CO_2 emissions in riparian wetlands (Fig. 6(a)) in August decreased from 2444.69 ± 228.58

257    $mg \cdot m^{-2} \cdot h^{-1}$ in the upstream area to 665.08 ± 347.57 $mg \cdot m^{-2} \cdot h^{-1}$ downstream, and the

258   corresponding values for October were 238.12 ± 48.20 $mg \cdot m^{-2} \cdot h^{-1}$ and 94.14 ± 7.67 $mg \cdot m^{-2} \cdot h^{-1}$.

259   However, in hillslope grasslands (Fig. 6(b)), CO_2 emissions exhibited no significant seasonality

260   between upstream and downstream areas, with the mean values of 1103.40 ± 190.44 $mg \cdot m^{-2} \cdot h^{-1}$

261   in August and 79.18 ± 24.52 $mg \cdot m^{-2} \cdot h^{-1}$ in October. In addition, CO_2 emissions in transect T5

262   were lower for both months, with the averages of 162.83 ± 149.15 $mg \cdot m^{-2} \cdot h^{-1}$ and 63.26 ± 12.40

263    $mg \cdot m^{-2} \cdot h^{-1}$ in August and October, respectively. The upstream riparian zones exhibited higher

264   CO_2 emissions (894.32 ± 868.47 $mg \cdot m^{-2} \cdot h^{-1}$) than their downstream counterparts ($621.14 \pm$

265   704.10 $mg \cdot m^{-2} \cdot h^{-1}$). However, mean CO_2 emissions showed no significant differences in

266   grasslands, averaging 524.16 ± 450.10 $mg \cdot m^{-2} \cdot h^{-1}$ upstream and 508.06 ± 534.77 $mg \cdot m^{-2} \cdot h^{-1}$

267   downstream.

268   CH_4 emissions showed a marked spatial pattern in the riparian zones from upstream to

269   downstream (Fig. 6(c)). The transects with continuous river flow were CH_4 sources in August and

270   October, with the average emissions of 1.42 ± 3.41 $mg \cdot m^{-2} \cdot h^{-1}$ and 0.27 ± 0.49 $mg \cdot m^{-2} \cdot h^{-1}$,

271   respectively, while those with intermittent river flow served as CH_4 sinks, with the corresponding

272   mean values of -0.21 ± 0.45 $mg \cdot m^{-2} \cdot h^{-1}$ and -0.02 ± 0.05 $mg \cdot m^{-2} \cdot h^{-1}$. Moreover, the hillslope

273   grassland sites in all transects were CH_4 sinks (Fig. 6(d)).

274   N_2O emissions in riparian wetlands (Fig. 7(e)) showed spatial patterns similar to those of

275   CH_4 emissions. In August, the transects with continuous river flow served as N_2O sources, with

276   the mean value of 0.031 ± 0.031 $mg \cdot m^{-2} \cdot h^{-1}$, while those with intermittent river flow were N_2O

277   sinks with an average value of -0.037 ± 0.05 $mg \cdot m^{-2} \cdot h^{-1}$. In October, N_2O emissions occurred as

278   weak sources in the longitudinal transects, averaging 0.002 ± 0.007 $mg \cdot m^{-2} \cdot h^{-1}$. However, N_2O

279   emissions in hillslope grasslands did not show any spatial pattern (Fig. 7(f)).

280

281   **4. Discussion**

282   **4.1 Main factors influencing GHG emissions**

283   4.1.1 Effects of SMC on GHG emissions

284   SMC constituted one of the main factors affecting GHG emissions in wetlands. In this study,

285   transects T1–T4 were characterized by a marked spatial SMC gradient (i.e., a gradual decrease

286   from the riparian wetlands to the hillslope grasslands, and from upstream to downstream (Fig. 3)).

287   The CO_2, CH_4, and N_2O emissions showed a similar trend. In Table 2, SMC10 is correlated with

288   CO_2 emissions ($P < 0.05$), SMC10 and SMC20 are significantly correlated with CH_4 emissions (P

289   < 0.01), and SMC10 and SMC20 are highly correlated with N_2O emissions ($P < 0.05$ and $P < 0.01$,

290   respectively). These results indicated the influence of wetland SMC on GHG emissions.

291   Typically, the optimal SMC values associated with CO_2 emissions in riparian wetlands range

292   from 40 to 60% (Sjögersten et al., 2006), and excessive SMC reduces soil gas transfer. On the

293   contrary, the SMC of hillslope grasslands is less than 10%, leading to a decrease in CO_2 emissions

294   compared to those in riparian zones (Moldrup et al., 2000). Similar results were obtained in our

295   study. The changes in CO_2 emissions in transect T5 were contrary to the change in the SMC likely

296   because other sediment properties for this transect were not conducive to the survival of

297   microorganisms (Table 1), and the increase in SMC did not increase the respiration activity of

298   microorganisms.

299   The largest CH_4 emissions were observed at the near-stream sites (i.e., L1 and R1) in T1, T2,

300   and T3, with the average SMC of 30.29%, while the SMC values at the other sites, which were

301   either weak sources or sinks, averaged at 14.57%. These results indicate that a higher SMC is

302   favorable for CH_4 emissions because a higher SMC denotes a soil in a reduced state, which is

303   beneficial for CH_4 production and inhibits CH_4 oxidation. A similar result was reported by Xu et al.

304   (2008). They conducted experiments of CH_4 emissions from a variety of paddy soils in China, and

305   showed that CH_4 production rates increased with the increase in SMC at the same incubation

306   temperature. Meng et al. (2001) also reported that water depth was the main factor affecting CH_4

307   emissions from wetlands. When the water level dropped below the soil surface, the decomposition

308   of organic matter accelerated, and CH_4 emissions decreased. If the oxide layer is large, the soil is

309   transformed into a CH_4 sink (Meng et al., 2011).

310   The N_2O fluxes showed a clear spatial pattern associated with the changes in SMC. When

311   SMC was below the saturated water content, N_2O emissions increased with the increase in SMC.

312   In contrast, when SMC was above the saturated water content, N_2O emissions gradually decreased

313   with the increase in SMC (Niu et al., 2017). In our study, N_2O emissions in the riparian wetlands

314   with a high SMC were higher than those in the hillslope grasslands, and N_2O emissions in the

315   upstream transects were higher than those downstream. These findings are consistent with those of

316   Liu et al. (2003), who showed that SMC is an essential factor affecting N_2O emissions.

317

318   4.1.2 Effects of ST on GHG emissions

319   ST was another important factor affecting the CO_2 emissions in this study, as this parameter

320   was significantly correlated with CO_2 emissions ($P < 0.01$) (Table 2). The activity of soil

321   microorganisms increases with rising soil temperatures, leading to increased respiration, and

322   consequently higher CO_2 emissions (Heilman et al., 1999). Previous studies reported that ST

323   partially controls seasonal CO_2 emission patterns (Inubushi et al., 2003). Therefore, CO_2

324   emissions in August were significantly higher than those in October in this study.

325   CH_4 emissions showed a clear seasonal pattern because high summer temperatures improve

326   the activity of both CH_4-producing and -oxidizing bacteria (Ding et al., 2010). In this study, ST

327   was closely related to CH_4 emissions, especially in the near-stream sites, and CH_4 emissions in

328   August were 59 times higher than those in October. Conversely, seasonal fluctuations in CH_4

329   emissions at the downstream sampling sites were small. Table 2 indicates that the correlation

330   between CH_4 emissions and temperature is not significant because the production and emission of

331   CH_4 are significantly affected by water conditions. SMC showed a positive correlation with GHG

332   emissions. In addition, SMC affected ST to a certain extent, while the interactions between SMC

333   and ST had a mutual influence on CH_4 emissions. During the study period, the near-stream sites

334   (L1 and R1) maintained a super-wet state on the ground surface for a long time, which was

335   beneficial for the production of CH_4. However, the wetlands maintained a state without water

336   accumulation on the soil surface in the growing season, which was conducive to the oxidative

337   absorption of CH_4. SMC thus masked the effect of ST on CH_4 emissions.

338   Previous studies indicated that temperature is an important factor affecting N_2O emissions

339   (Sun et al., 2011) through primary mechanisms impacting the activities of the nitrifying and

340   denitrifying bacteria in soil. Table 2 shows that the correlations between N_2O emissions and ST10

341   and ST20 are poor ($P > 0.05$). This can be attributed to the wide suitable temperature range for

342   nitrification-denitrification and weak sensitivity to temperature. The average ST in August was

343   27.4°C, conducive to the growth of denitrifying microorganisms, while that in October was

344   8.97°C, and the microbial activity was generally low (Sun et al., 2011). Furthermore, ST

345   fluctuations were low   both in August and October. Therefore, the effect of ST on N_2O emissions

346   was masked by other factors, such as moisture content.

347

348   4.1.3 Effects of BIO and soil organic matter on GHG emissions

349   CO_2 and CH_4 emissions were higher in the riparian wetlands than in the grasslands, mainly

350   because of greater vegetation cover. Typically, CO_2 emissions from riparian wetlands originate

351   from plants and microorganisms, with plant respiration accounting for a large proportion in the

352   growing season. Previous studies have shown that plant respiration accounts for 35–90% of the

353   total respiration in the wetland ecosystem (Johnson-Randall and Foote, 2005). Good soil

354   physicochemical properties and high soil total organic carbon (TOC) of riparian wetlands improve

355   the activity of soil microorganisms and plant root respiration. Table 2 shows that BIO is

356   significantly correlated with the CO_2 ($P < 0.05$) and CH_4 ($P < 0.01$) emissions. These results can

357   be attributed to the significant linear positive correlation between the respiration rate and plant

358   biomass (Lu et al., 2007). Higher plant biomass storage can achieve more carbon accumulation

359   during photosynthesis and higher exudate release by the roots. This, in turn, promotes the

360   accumulation of soil organic matter. Increased amount of organic matter stimulates the growth and

361   reproduction of soil microorganisms, ultimately promoting CO_2 and CH_4 emissions. Moreover,

362   plants act as a gas channel for CH_4 transmission, and a larger amount of biomass promotes CH_4

363   emissions, given the increased number of channels. In transect T3, high CO_2 emissions observed

364   at site L3 can be attributed to the relatively high levels of SMC, BIO, and soil nutrients, which

365   stimulate the microbial respiration rates.

366   BIO had a weak correlation with N_2O emissions (Table 2), which indicates that plants

367   increase N_2O production and emissions, although this may not be the most critical factor. Previous

368   studies reported mechanisms wherein the plants can absorb N_2O produced in the soil through the

369   root system before releasing it into the atmosphere. Additionally, the root exudates of plants can

370   enhance the activity of nitrifying and denitrifying bacteria in the soil, ultimately promoting the

371   production of N_2O. Finally, oxygen stress caused by plant respiration can regulate the production

372   and consumption of N_2O in the soil, eventually affecting the conversion of nitrogen in the soil

373   (Koops et al., 1996; Azam et al., 2005).

374   Site L3 in transect T3 was covered by tall reeds, and its BIO was much higher than those of

375   the other sites; thus, the data for this site were excluded from the correlation analysis.

376
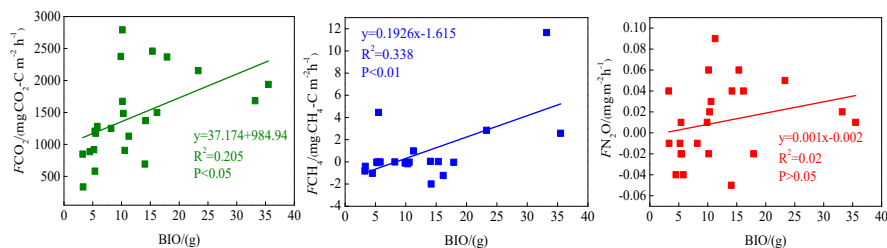
Fig. 7 Correlation between aboveground biomass (BIO) and GHG emissions (F)

379

380   The soil C:N ratio refers to the ratio of biodegradable carbonaceous organic matter and

381   nitrogenous matter in the soil, and it forms the soil matrix with TOC. TOC decomposition

382   provides energy for microbial activity, while the C:N ratio affects the decomposition of organic

383   matter by soil microorganisms (Gholz et al., 2010). The correlation results (Fig. 8) indicate that

384   TOC has a weak correlation with CO_2 emissions ($P > 0.05$), a poor correlation with CH_4 emissions

385   ($P > 0.05$), and a significant correlation with N_2O emissions ($P < 0.05$). Organic carbon provides a

386   carbon source for the growth of plants and microorganisms, which in turn boosts their respiration.

387   Moreover, as the abundance of heterotrophic nitrifying bacteria increases, soils become more

388   anaerobic, slowing down the growth of autotrophic nitrifying bacteria. This reduces the

389   nitrification rate, ultimately promoting N_2O release. Typically, low soil C:N ratios are favorable

390   for the decomposition of microorganisms, the most suitable range being between 10 and 12

391   (Pierzynski et al., 1994). Table 2 shows that N_2O emissions are significantly related to the soil C:N

392   ratios ($P < 0.05$), which means that denitrifying bacteria will use their own endogenous carbon

393   source for denitrification when the external carbon source is insufficient. Moreover, incomplete

394   denitrification leads to the accumulation of NO_2-N, which is conducive to the N_2O release. In this

395   study, all the sites in transects T1–T4 exhibited similar soil C:N ratios in the optimum range (Table

396   1), which is favorable for microbial decomposition. However, the soil C:N ratios in transect T5

397   were higher than those in the other transects, especially in the dry lake bed. Therefore, transect T5

398   showed severe mineralization and a low microbial decomposition rate.

399
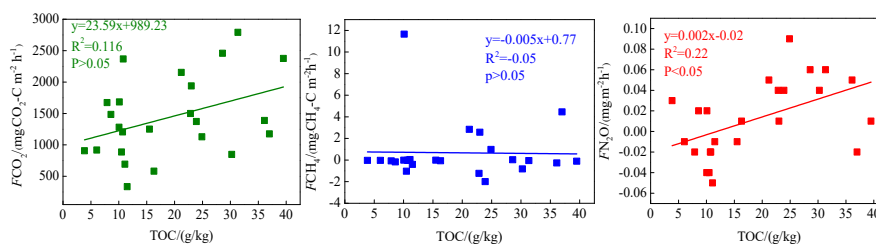
401   Fig. 8 Correlations between soil organic carbon (TOC) and GHG emissions (F)

402

403   Table 2. Correlations between CO_2, CH_4, and N_2O emissions and impact factors ($n = 62$)

GHG flux	ST10	ST20	SMC10	SMC20	TOC	ρ_b	C:N	pH	EC	BIO
CO_2	0.634**	0.592**	0.307*	0.216	0.393	−0.463**	−0.289*	−0.350**	−0.251*	0.491*
CH_4	−0.029	−0.051	0.346**	0.353**	−0.02	−0.129	−0.156	−0.127	−0.107	0.607**
N_2O	0.127	0.118	0.304*	0.356**	0.493*	−0.194	0.311*	0.137	0.504**	0.251

404   Note: 1. * and ** denote significant and highly significant correlations ($P < 0.01$ and $P < 0.05$),

405   respectively.

406   2. ST - soil temperature, SMC - soil moisture content, ρ_b - soil bulk density, soil C:N - soil

407   carbon-nitrogen ratio, pH - soil pH, EC - soil electrical conductivity, BIO - aboveground biomass

408

409   **4.2 Riparian wetlands as hotspots of GHG emissions**

410   The results of this study emphasized that CO_2 emissions in the riparian wetlands were higher

411   than those in the hillslope grasslands owing to a variety of factors. ST is an important factor

412   affecting GHG emissions. Mclain and Martens (2006) showed that seasonal fluctuations in ST and

413   SMC in semi-arid regions have important effects on CO_2, CH_4, and N_2O emissions in riparian

414   soils. Poblador et al. (2017) studied the GHG emissions in forest riparian zones and suggested that

415   the difference in the CO_2 and N_2O emissions in these zones is affected by the spatial gradient of

416   the regional SMC. In this study, the upstream riparian wetlands are characterized by higher TOC,

417   lower soil C:N ratio, and abundant BIO than the hillslope grasslands (Table 1). These soil

418   conditions benefited the soil microbial activity, ultimately enhancing respiration as well as CO_2

419   emissions. However, CO_2 emissions in downstream areas were nearly identical to those in the

420   grasslands because the wetlands gradually evolved into grasslands after their degradation. The

421   N_2O emissions showed spatial patterns similar to those of the CO_2 emissions because the CO_2

422   concentrations were closely related to the processes of nitrification and denitrification, and high

423   CO_2 concentrations can promote the carbon and nitrogen cycles in soil (Azam et al., 2005; Baggs

424   et al., 2003), providing the substrate and energy required for the nitrification and denitrification

425   reactions. Moreover, soil respiration increases during soil denitrification (Liu et al., 2010;

426   Christensen et al., 1990). In this study, a weak correlation was observed between the CO_2 and CH_4

427   emissions in the riparian zones ($r = 0.228$), but CO_2 emissions were significantly correlated with

428   N_2O emissions ($r = 0.322$, $P < 0.05$). The soil became anaerobic in the riparian areas as the SMC

429   increased, and this was conducive to the survival of CH_4-producing bacteria and denitrification

430   reactions, eventually leading to an increase in CH_4 and N_2O emissions. Jacinthe et al. (2015)

431   reported that inundated grassland-dominated riparian wetlands were CH_4 sinks (-1.08 ± 0.22

432    $kg \cdot CH_4\text{-}C \ ha^{-1} \cdot yr^{-1}$), but Lu et al. (2015) indicated that grasslands were CH_4 sinks. In our study, a

433   marked water gradient across the transects led to the transformation of the soil from anaerobic to

434   aerobic soil, which changed the wetland function as a CH_4 source or sink. Therefore, during the

435   transition from the riparian wetlands to the hillslope grasslands, CH_4 emissions only appeared as

436   sources in the near-stream sites and sinks at other sites.

437   Further, we compared the GHG emissions of riparian wetlands and hillslope grasslands

438   around the Xilin River Basin with various types of grasslands (meadow grassland, typical

439   grassland, and desert grassland) in the Xinlingol League in Inner Mongolia (Table 3). The CO_2

440   emissions in August decreased in the following order: upstream riparian wetlands > downstream

441   riparian wetlands > hillslope grasslands > meadow grassland > typical grassland > desert

442   grassland. Moreover, the upper riparian wetlands acted as the source of CH_4 emissions, while the

443   downstream transects and grasslands served as CH_4 sinks. Similarly, except for the downstream

444   transects, N_2O emissions occurred as weak sources in different types of grasslands and upstream

445   riparian wetlands. The GHG emissions showed similar spatial patterns in October. Although these

446   estimates were made only in the growing season in August and the non-growing season in October,

447   our results suggest that riparian wetlands are the potential hotspots of GHG emissions. Thus, it is

448　important to study GHG emissions to obtain a comprehensive picture of the role of riparian

449　wetlands in climate change.

450

451　　　　　　　　Table 3. GHG emission fluxes of riparian wetlands and grasslands

Sample plot	GHG emissions in August ($mg \cdot m^{-2} \cdot h^{-1}$)			GHG emissions in October ($mg \cdot m^{-2} \cdot h^{-1}$)			Reference
	CO_2	CH_4	N_2O	CO_2	CH_4	N_2O	
Wetlands of upstream transects (T1, T2, and T3)	1606.28	1.417	0.031	182.35	0.272	0.002	
Wetlands of downstream transects (T4 and T5)	1144.15	−0.215	−0.037	98.13	−0.015	0.001	This study
Hillslope grasslands of all transects	1103.40	−0.246	0.001	79.18	−0.048	−0.002	
Meadow grassland	166.39	−0.038	0.002	-	-	-	
Typical grassland	240.32	−0.042	0.037	-	-	-	Guo et al., 2017
Desert grassland	107.59	−0.036	0.003	-	-	-	
Typical grassland	520.25	−0.102	0.007	88.34	−0.099	0.005	Zhang, 2019
Typical grassland	232.42	−0.090	0.004	-	-	-	Chao, 2019
Typical grassland	265.23	−0.185	0.005	189.41	−0.092	0.004	
Meadow grassland	553.85	−0.163	0.003	47.73	−0.019	0.011	Geng, 2004
Typical grassland	308.60	−0.105	0.002	70.25	−0.029	0.007	

452

4.3 Effects of riparian wetland degradation on GHG emissions

454　　　　The hydrology and soil properties showed more evident differences among the transects

455　because the downstream zone was dry all year due to the presence of the Xilinhot Dam (Fig. 1).

456　The dam caused the degradation of the riparian wetlands, resulting in reduced GHG emissions.

457　The average CO_2 emissions amounted to 1663 $mg \cdot m^{-2} \cdot h^{-1}$ in the riparian wetlands in the upstream

458　transects (T1, T2, and T3), while the downstream transects (T4 and T5) recorded an average of

459   1084 $mg \cdot m^{-2} \cdot h^{-1}$, 35% lower than the value in the upstream transects. The N_2O emissions from

460   the riparian wetlands were lower in the downstream transects.

461   The wetland degradation first resulted in the continuous reduction of SMC, affecting the

462   wetland carbon cycle processes. When the soil environment became less moist and more aerobic,

463   the CH_4 and N_2O emissions changed as the environment was transformed from a source to a sink,

464   and CO_2 emissions decreased. Table 1 shows that soil TOC in the upstream transects (average:

465   25.1 $g \cdot kg^{-1}$) is higher than that in the downstream transects (average: 8.41 $g \cdot kg^{-1}$). This result

466   indicates that wetland degradation caused the loss of the soil carbon pool and weakened the

467   wetland carbon source/sink function. These results are in agreement with those of Xia (2017).

468   The relatively low SMC and the aerobic environment were conducive to the mineralization

469   and decomposition of TOC. The degradation of plants in the wetlands led to the gradual reduction

470   of BIO. Ultimately, the plant carbon source input of the degraded wetlands decreased and the bare

471   land temperature increased due to the reduced plant shelter. This accelerated the decomposition of

472   TOC, leading to its decrease.

473   The degraded wetlands also caused soil desertification and salinization, leading to a decline

474   in the physical protection afforded by organic carbon and a reduction in soil aggregates. Thus, the

475   preservation provided by organic carbon declined. Soil TOC and SMC in the dry lake bed in

476   transect T5 were relatively high, but GHG emissions were very low along this transect because

477   soil pH values increased after the degradation of the lake soil, exceeding the optimum range

478   required for microorganism activity. The soil C:N ratio was very high, resulting in severe

479   mineralization and a low microbial decomposition rate, hence affecting the GHG emissions.

480

481   **5. Conclusions**

482   The riparian wetlands in the Xilin River Basin constitute a dynamic ecosystem. The present

483   spatial and temporal transfers in the studied biogeochemical processes were attributed to the

484   changes in SMC, ST, and soil substrate availability. Our simultaneous analysis of CO_2, CH_4, and

485   N_2O emissions from riparian wetlands and hillslope grasslands in the Xilin River Basin revealed

486   that the majority of the GHG emissions occurred in the form of CO_2. Moreover, our results clearly

487   illustrated a marked seasonality and spatial pattern of GHG emissions along the transects and in

488   the longitudinal direction (i.e., upstream and downstream). SMC and ST were two critical factors

489 controlling the GHG emissions. Moreover, abundant BIO promoted the CO_2, CH_4, and N_2O

490 emissions.

491 The riparian wetlands were the potential hotspots of GHG emissions in the Inner Mongolian

492 region. However, the degradation of wetlands transformed the area from a source to a sink for CH_4

493 and N_2O emissions, and reduced CO_2 emissions, which severely affected the wetland carbon cycle

494 processes. Overall, our study suggests that anthropogenic activities have significantly changed the

495 hydrological characteristics of the studied area, and will accelerate carbon loss from the riparian

496 wetlands and further influence the GHG emissions in the future.

Author Contributions

498 Xinyu Liu, Xixi Lu and Ruihong Yu designed the research framework and wrote the

499 manuscript. Xixi Lu and Ruihong Yu supervised the study. Xinyu Liu, Hao Xue, Zhen Qi,

500 Zhengxu Cao and Zhuangzhuang Zhang carried out the field experiments and laboratory

501 experiments analyses. Z.Z. drew GIS mapping in this paper. Tingxi Liu proofread the manuscript.

Acknowledgements

Competing interests

508 The authors declare no conflicts of interest.

References

510 Azam F., Gill S., Farooq S.: Availability of CO_2 as a factor affecting the rate of nitrification in soil,

511 Soil Biology & Biochemistry, 37, 2141–2144, doi 10.1016/j.soilbio.2005.02.036, 2005.

512 Baggs E.M., Richter M., Cadisch G., Hartwig U.A.: Denitrification in grass swards is increased

513 under elevated atmospheric CO_2, Soil Biology and Biochemistry, 35, 729–732, doi

514 10.1016/S0038-0717(03)00083-X, 2003

515 Beger M., Grantham H.S., Pressey R.L., Wilson K.A., Peterson E.L., Dorfman D., Lourival R.,

516 Brumbaugh D.R., Possingham H.P.: Conservation planning for connectivity across marine,

517 freshwater, and terrestrial realms, Biological Conservation, 143, 565–575, doi

518 10.1016/j.biocon.2009.11.006, 2010.

519   Cao M., Yu G., Liu J., Li K.; Multi-scale observation and cross-scale mechanistic modelling on

520   terrestrial ecosystem carbon cycle, Science in China Ser. D Earth Sciences, 48, 17–32, doi

521   10.1360/05zd0002, 2005.

522   Chao R.: Effects of Simulated Climate Change on Greenhouse Gas Fluxes in Typical Steppe

523   Ecosystem, Inner Mongolia University, 2019.

524   Cheng S and Huang J.: Enhanced soil moisture drying in transitional regions under a warming

525   climate, Journal of Geophysical Research-Atmospheres, 121, 2542–2555, doi

526   10.1002/2015JD024559, 2016.

527   Christensen S., Simkins S., Tiedje J M.: Temporal Patterns of Soil Denitrification: Their Stability

528   and Causes, Soil Science Society of America Journal, 54, 1614, doi

529   10.2136/sssaj1990.03615995005400060017x, 1990.

530   Ding W., Cai Z., Tsuruta H.: Cultivation, nitrogen fertilization, and set‐aside effects on methane

531   uptake in a drained marsh soil in Northeast China, Global Change Biology, 10, 1801–1809, doi

532   10.1111/j.1365-2486.2004.00843.x, 2010.

533   Ferrón S., Ortega T., Gómez-Parra A., Forja J.M.: Seasonal study of dissolved CH_4, CO_2 and N_2O

534   in a shallow tidal system of the bay of Cádiz (SW Spain), Journal of Marine Systems, 66, 244–257,

535   doi 10.1016/j.jmarsys.2006.03.021, 2007.

536   Geng H.: Study on Charactors of CO_2, CH_4, N_2O Fluxes and the Relationship between Them and

537   Environmental Factors in the Temperate Typical Grassland Ecosystem, Northwest Agriculture &

538   Forestry University, 2004.

539   Gholz H.L., Wedin D.A., Smitherman S.M., Harmon M.E., Parton W.J.: Long-term dynamics of

540   pine and hardwood litter in contrasting environments: toward a global model of decomposition,

541   Global Change Biology, 6, 751–765, doi 10.1046/j.1365-2486.2000.00349.x, 2000.

542   Gou Q., Qu J., Wang G., Xiao J., Pang Y.: Progress of wetland researches in arid and

543   semi-ariregions in China, Arid Zone Research, 1001–4675, 213–220, 2015.

544   Guo X., Zhou D., Li Y.: Net Greenhouse Gas Emission and Its Influencing Factors in Inner

545   Mongolia Grassland, Chinese Grassland Society, 2017.

546   Heilman J.L., Cobos D.R., Heinsch F.A., Campbell C.S., McInnes K.J.: Tower-based conditional

547   sampling for measuring ecosystem-scale carbon dioxide exchange in coastal wetlands, Estuaries,

548   22, 584–591, doi 10.2307/1353046, 1999.

549   Inubushi K., Furukawa Y., Hadi A., Purnomo E., Tsuruta H.: Seasonal changes of CO_2, CH_4 and

550   N_2O fluxes in relation to land-use change in tropical peatlands located in coastal area of South

551   Kalimantan, Chemosphere, 52, 603–608, doi 10.1016/s0045-6535(03)00242-x, 2003.

552   IPCC.: Climate Change 2013: The Physical Science Basis. Contribution of Working, Working

553   Group I of the IPCC, 43, 866–871, 2013.

554   Jacinthe P.A., Vidon P., Fisher K., Liu X., Baker M.E.: Soil Methane and Carbon Dioxide Fluxes

555   from Cropland and Riparian Buffers in Different Hydrogeomorphic Settings, Journal of

556   Environment Quality, 44, 1080–1115, doi 10.2134/jeq2015.01.0014, 2015.

557   Johnson-Randall L.A., Foote A.L.: Effects of managed impoundments and herbivory on wetland

558   plant   production   and   stand   structure,   Wetlands,   25,   38–50,   doi

559   10.1672/0277-5212(2005)025[0038:eomiah]2.0.co;2, 2005.

560   Koops J.G., Oenema O., Beusichem M.L.: Denitrification in the top and sub soil of grassland on

561   peat soils, Plant and Soil, 184, 1–10, doi 10.1007/bf00029269, 1996.

562   Kou X.: Study on Soil Physicochemical Properties and Bacterial Community Characteristics of

563   River Riparian Wetland in Inner Mongolia Grassland, Inner Mongolia University, 2018.

564   Liu J., Wang J., Li Z., Yu J., Zhang X., Wang C., Wang Y.: N_2O Concentration and Its Emission

565   Characteristics in Sanjiang Plain Wetland, Chinese Journal of Environmental Science, 24, 33–39,

566   2003.

567   Liu C., Xie G., Huang H.: Shrinking and drying up of Baiyangdian Lake wetland: a natural or

568   human cause? Chinese Geographical Science, 16, 314–319, 2006.

569   Liu F., Liu C., Wang S., Zhu Z.: Correlations among CO_2, CH_4, and N_2O concentrations in soil

570   profiles in central Guizhou Karst area, Chinese Journal of Ecology, 29, 717–723, doi

571   10.1016/S1872-5813(11)60001-7, 2010.

572   Lu Y., Song C., Wang Y., Zhao Z.: Influence of plants on CO_2 and CH_4 emission in wetland

573   ecosystem, Acta Botanica Boreali-Occidentalia Sinica, 27, 2306–2313, 2007.

574   Lu Z., Du R., Du P., Li Z., Liang Z., Wang Y., Qin S., Zhong L.: Effect of mowing on N_2O and

575   CH_4 fluxes emissions from the meadow-steppe grasslands of Inner Mongolia, Frontiers of Earth

576   Science, 9, 473–486, doi 10.1007/s11707-014-0486-z, 2015.

577   Lv M., Sheng L., Zhang L.: A review on carbon fluxes for typical wetlands in different climates of

578   China, Wetland Science, 11, 114–120, doi CNKI:SUN:KXSD.0.2013-01-020, 2013.

579   Mclain J E T., Martens D.A.: Moisture controls on trace gas fluxes in semiarid riparian soils, Soil

580   Science Society of America Journal, 70, 367, doi 10.2136/sssaj2005.0105, 2006.

581   Meng W., Wu D., Wang Z.: Control factors and critical conditions between carbon sinking and

582   sourcing of wetland ecosystem, Ecology and Environmental Sciences, 20, 1359–1366, doi

583   10.1016/S1671-2927(11)60313-1, 2011.

584   Mitsch W.J., Gosselink J.G.: Wetlands (Fourth Edition), John Wiley & Sons Inc.: Hoboken, New

585   Jersey, USA, 2007.

586   Mitsch W.J., Gosselink J.G., Anderson C.J., Anderson, C. J.: Wetland ecosystems: John Wiley &

587   Sons, 2009.

588   Moldrup P., Olesen T., Schjønning P., Yamaguchi T., Rolston D.E.: Predicting the gas diffusion

589   coefficient in undisturbed soil from soil water characteristics, Soil Science Society of America

590   Journal, 64, 1588–1594, doi 10.2136/sssaj2000.64194x, 2000.

591   Naiman R.J., Decamps H.: The ecology of interfaces: Riparian zones, Annual Review of Ecology

592   & Systematics, 28, 621–658, doi 10.2307/2952507, 1997.

593   National Agricultural Technology Extension Service Center (NATESC).: Technical specification

594   for soil analysis, 2006.

595   Niu C., Wang S., Guo Y., Liu W., Zhang J.: Studies on variation characteristics of soil nitrogen

596   forms, nitrous oxide emission and nitrogen storage of the Phragmites australis-dominated

597   land/inland water ecotones in Baiyangdian wetland, Journal of Agricultural University of Hebei,

598   40, 72–79, 2017.

599   Pierzynski G M S., J.T.,Vance, G.F.: Soils and Environmental Quality, 1994.

600   Poblador S., Lupon A., Sabaté S., Sabater F.: Soil water content drives spatiotemporal patterns of

601   CO_2 and N_2O emissions from a Mediterranean riparian forest soil, Biogeosciences Discussions, 14,

602   1–28, doi 10.5194/bg-14-4195-2017, 2017.

603   Qin S., Tang J., Pu J., Xu Y., Dong P., Jiao L., Guo J.: Fluxes and influencing factors of CO_2 and

604   CH_4 in Hangzhou Xixi Wetland，China, Earth and Environment, 44, 513–519, 2016.

605   Sjögersten S., Wal R V.D., Woodin S.J.: Small-scale hydrological variation determines landscape

606   CO_2 fluxes in the high Arctic, Biogeochemistry, 80, 205–216, doi 10.2307/20456398, 2006.

607   Sun Y., Wu H., Wang Y.: The influence factors on N_2O emissions from nirification and

608   denitrification   reaction,   Ecology   and   Environmental   Sciences,   20,   384–388,   doi

609   10.1631/jzus.B1000275, 2011.

610   Tong C., Wu J., Yong S., Yang J., Yong W.: A landscape-scale assessment of steppe degradation in

611   the Xilin River Basin, Inner Mongolia, China, Journal of Arid Environments, 59, 133–149, doi

612   10.1016/j.jaridenv.2004.01.004, 2004.

613   Waddington J.M., Roulet N.T.: Carbon balance of a boreal patterned peatland, Global Change

614   Biology, 6, 87–97, doi 10.1046/j.1365-2486.2000.00283.x, 2000.

615   WMO.: WMO Statement on the State of the Global Climate in 2017, World Meteorological

616   Organization, 2018.

617   Xi X., Zhu Z., Hao X.: Spatial variability of soil organic carbon in Xilin River Basin, Research of

618   Soil and Water Conservation, 24, 97–104, 2017.

619   Xia P., Yu L., Kou Y., Deng H., Liu J.: Distribution characteristics of soil organic carbon and its

620   relationship with enzyme activity in the Caohai wetland of the Guizhou Plateau, Acta Scientiae

621   Circumstantial, 37, 1479–1485, doi 10.13671/j.hjkxxb.2016.0129, 2017.

622   Xu H., Cai Z., Yagi K.: Methane Production Potentials of Rice Paddy Soils and Its Affecting

623   Factors, Acta Pedologica Sinica, 45, 98–104, doi 10.1163/156939308783122788, 2008.

624   Zhang D.: Effects of Different Grazing Intensities on Greenhouse Gases Flux in Typical Steppe of

625   Inner Mongolia, Inner Mongolia University, 2019.

626   Zona D., Oechel W.C., Kochendorfer J., Paw U K.T., Salyuk A.N., Olivas P.C., Oberbauer S.F.,

627   Lipson D.A.: Methane fluxes during the initiation of a large-scale water table manipulation

628   experiment in the Alaskan Arctic tundra, Global Biogeochem Cycles, 23, doi

629   10.1029/2009gb003487, 2009.